

CrossMark
click for updates

Cite this: DOI: 10.1039/c7cy00088j

The selective oxidation of substituted aromatic hydrocarbons and the observation of uncoupling *via* redox cycling during naphthalene oxidation by the CYP101B1 system†

Emma A. Hall, Md Raihan Sarkar and Stephen G. Bell*

The cytochrome P450 monooxygenase enzyme CYP101B1, from *Novosphingobium aromaticivorans* DSM12444, efficiently and selectively oxidised a range of naphthalene and biphenyl derivatives. Methyl substituted naphthalenes were better substrates than ethylnaphthalenes and naphthalene itself. The highest product formation activity for a singly substituted alkylnaphthalene was obtained with 2-methylnaphthalene. The oxidation of alkylnaphthalenes was regioselective for the benzylic methyl or methine C–H bonds. The products from 1- and 2-ethylnaphthalene oxidation were highly enantioselective with a single stereoisomer being generated in significant excess. The disubstituted substrate, 2,7-dimethylnaphthalene, had a higher product formation activity than either 1- and 2-methylnaphthalene. Methyl substituted biphenyls were also better substrates than biphenyl and had similar biocatalytic parameters to 1-methylnaphthalene. CYP101B1 catalysed oxidation of 2- and 3-methylbiphenyl was selective for attack at the methyl C–H bonds. The exception was the turnover of 4-methylbiphenyl which generated 4'-(4-methylphenyl)phenol as the major product (70%) with 4-biphenylmethanol making up the remainder. The drug molecule diclofenac was also regioselectively oxidised to 4'-hydroxydiclofenac by CYP101B1. The activity of the CYP101B1 system with naphthalene was more complex and the rate of NADH oxidation increased over time but very little product, 1-naphthol, was generated. Addition of samples of 1-naphthol and 2-naphthol and low concentrations of 1,4-naphthoquinone induced rapid NADH oxidation activity in the *in vitro* turnovers in both the presence and absence of the cytochrome P450 enzyme. Hydrogen peroxide was generated in these reactions in absence of the P450 enzymes demonstrating that the ferredoxin and ferredoxin reductase in combination with quinones from naphthol oxidation and oxygen can undergo redox cycling giving rise to a form of uncoupling of the reducing equivalents.

Received 16th January 2017,
Accepted 9th March 2017

DOI: 10.1039/c7cy00088j

rsc.li/catalysis

Introduction

There is great interest in applying cytochrome P450 (CYP) enzymes as biocatalysts for the regio- and stereo-selective insertion of an oxygen atom into chemically inert carbon–hydrogen bonds.^{1–7} This monooxygenase activity requires two electrons that are usually derived from NAD(P)H and these are delivered one at a time, as required, to the CYP enzymes by electron transfer proteins.⁸ Electron transfer is often the rate determining step in CYP catalysis and the activities of many CYP enzymes are compromised when alternative electron transfer systems are used.^{9–11} In addition uncoupling reactions which can arise from poor enzyme/substrate compatibil-

ity and leakage due to oxygen reduction competing with slow inter-protein electron transfer can reduce the effectiveness of the enzyme. Both result in oxygen reduction without product formation.^{12–14} The identification and application of highly active monooxygenase systems greatly facilitates biocatalytic C–H bond oxidation of hydrocarbons and aromatics.^{15–17} Therefore the isolation and characterisation of new complete systems which are capable of performing challenging reactions, such as the selective oxidation of aromatic molecules, is of paramount importance in the field of fine chemical synthesis.

Many bacterial and fungal monooxygenase enzymes have been investigated as potential biocatalysts for the oxidation of aromatic molecules.^{18–20} The fungal peroxygenases from *Agrocybe aegerita* and *Coprinellus radians* were able to oxidise a broad range of polyaromatic hydrocarbons.²¹ Certain members of the self-sufficient CYP102 family of P450 monooxygenases, which are highly active for fatty acid substrates,

Department of Chemistry, University of Adelaide, SA 5005, Australia.

E-mail: Stephen.bell@adelaide.edu.au

† Electronic supplementary information (ESI) available: Additional data, chromatograms, MS and NMR data. See DOI: 10.1039/c7cy00088j

have activity with aromatic substrates.^{2,16} CYP102A1, from *Bacillus megaterium*, has been modified *via* protein engineering to facilitate the oxidation of aromatic substrates such as naphthalene, phenanthrene and pyrene.^{2,22} Class I CYP enzymes, such as CYP101A1 (P450cam), from a *Pseudomonas* sp., whose electron transfer systems consist of a flavin-dependent ferredoxin reductase and a ferredoxin, are also capable of high monooxygenase activities and selective oxidations.^{11,23,24} The wild-type forms of various class I CYP enzymes and mutants of CYP101A1, have been reported to be biocatalysts for the oxidation of aromatic molecules including polyaromatic hydrocarbons and biphenyl.^{25–29}

Naphthalene, methylnaphthalenes and substituted biphenyls are toxic molecules which are ubiquitous in the environment.³⁰ Substituted naphthalene and biphenyl derivatives are also found in a range of molecules with pharmacological activity including drug molecules such as diflunisal, naftifine, terbinafine and tolnaftate. The enzyme catalysed oxidation of these aromatic substrates has potential applications in environmental bioremediation and fine chemical synthesis. The Phe87Val mutant form of CYP102A1 has been used to oxidise naphthalene derivatives, including the methyl and dimethyl substituted forms.³¹ CYP110E1, from *Nostoc* sp. strain PCC7120, oxidised substituted naphthalenes and biphenyls.³² The reducing equivalents were provided to CYP110E1 by fusing the enzyme to the RhFred reductase domain of CYP116B2 from *Rhodococcus* sp. NCIMB 9784.³³ The turnovers of substituted naphthalenes by both of these monooxygenase enzymes were generally not selective with at least two products being generated in low yields for each substrate.^{31,32} The fungal peroxygenases from *Agrocybe aegerita* and *Coprinellus radians* efficiently oxidised 1- and 2-methylnaphthalene unselectively to numerous products including those arising from multiple oxidations.³⁴

Novosphingobium bacteria are able to degrade a variety of aromatic hydrocarbons and therefore the oxygenase enzymes from these species have the potential to be biocatalysts for the oxidation of these hydrophobic substrates.^{35,36} The bacterium *Novosphingobium aromaticivorans* DSM12444 contains many monooxygenase and dioxygenase enzyme coding genes.³⁵ The cytochrome P450 monooxygenase CYP108D1 from *N. aromaticivorans* has been shown to bind biphenyl, naphthalene, phenanthrene and phenylcyclohexane.²⁰ CYP101B1 from the same bacterium, which is related to CYP101A1, CYP101C1, CYP101D1 and CYP101D2 (the last three also being from *N. aromaticivorans*), oxidised indole generating indigo.^{11,37–39} We have reported that the CYP101B1 enzyme is an active biocatalyst for the oxidation of norisoprenoids and can turnover other structurally diverse substrates including phenylcyclohexane and various esters.^{37,40–44} Importantly a class I electron transfer system, consisting of a flavin-dependent ferredoxin reductase, ArR, and a [2Fe–2S] ferredoxin, Arx, has been identified from this bacterium. This electron transfer system supports the activity of CYP101B1, as well as those of CYP101D1, CYP101D2, CYP101C1 and CYP111A2 but not that of

CYP108D1.^{11,20,37,40,41} The product formation activity with the best substrates is in excess of 1000 nmol nmol P450^{–1} min^{–1}. A whole-cell system containing CYP101B1, ArR and Arx, which is capable of product formation on the gram-per-liter scale in shake flasks, has been constructed.³⁷ Therefore CYP101B1 is a promising monooxygenase system for biocatalytic applications involving C–H bond oxidation reactions.

Aromatic molecules including phenylcyclohexane and *p*-cymene have been oxidised by CYP101B1 with the activity of phenylcyclohexane oxidation being five times higher than the oxidation of *p*-cymene.⁴¹ Phenylcyclohexane was selectively oxidised to *trans*-4-phenylcyclohexanol while *p*-cymene was hydroxylated at the benzylic carbons to yield a mixture of isopropylbenzyl alcohol and *p*- α,α -trimethylbenzylalcohol. Despite inducing a lower shift to the high spin form ($\leq 20\%$) compared to norisoprenoids, phenylcyclohexane binds to CYP101B1 with comparable affinity to β -damascone suggesting that larger two ring aromatic systems may be good substrates for this enzyme.⁴¹ Many drug molecules contain multiple aromatic rings and the identification and synthesis of drug metabolites using soluble and highly active P450 enzymes could simplify the drug development process. Here we report that the substrate range of CYP101B1 includes aromatic substrates and demonstrate it is capable of acting as a biocatalyst for the oxidation of substituted naphthalenes, biphenyls and the drug molecule diclofenac. During these investigations we determined that the oxidation products of naphthalene could interfere with the transfer of the electrons from the ferredoxin to the P450 enzyme which provided an alternate mechanism for uncoupling *via* unproductive redox cycling in these systems.

Experimental

General

General reagents and organics were from Sigma-Aldrich, TCI, Acros or VWR. Buffer components (Tris–HCl) NADH, and isopropyl- β -D-thiogalactopyranoside (IPTG) were from Anachem (Astral Scientific, Australia) or Biovectra, (Scimar, Australia). General DNA manipulations and microbiological experiments and the expression, purification and quantitation of CYP101B1 and the electron transfer proteins ArR and Arx from *N. aromaticivorans* were each performed as described previously.^{37,40} All the proteins were purified to $\geq 90\%$ by two ion-exchange steps.^{37,40}

Substrate binding and kinetic analysis

UV/vis spectroscopy was performed on Varian Cary 5000 or Agilent Cary 60 spectrophotometers. For substrate binding the P450 enzymes were diluted to ~ 3.5 – $10 \mu\text{M}$ using 50 mM Tris, pH 7.4. After addition of the substrate (as 1 μL aliquots from a 50 mM stock in DMSO or ethanol) the high spin heme content was estimated, to approximately $\pm 5\%$, by comparison with a set of spectra generated from the sum of the appropriate percentages of the spectra of the substrate-free form ($>95\%$ low spin, Soret maximum at 418 nm) and camphor-

bound form (>95% high spin, Soret maximum at 392 nm) of wild-type CYP101A1.

To determine the dissociation constants of CYP101B1 with the aromatic substrates the enzyme was diluted to 1.6–3.7 μM in a total volume of 2.5 mL in 50 mM Tris, pH 7.4 and used to baseline the spectrophotometer. Aliquots of the substrate (0.5–2 μL) were added using a Hamilton syringe from a 1, 10, 50 or 100 mM stock solution in DMSO or EtOH. The solution was mixed and the peak-to-trough difference in absorbance recorded between 700 nm and 250 nm. Further aliquots of substrate were added until the peak-to-trough difference of the Soret band did not shift further. The apparent dissociation constant, K_d , was obtained by fitting the peak-to-trough difference against substrate concentration to a hyperbolic function (eqn (1)):

$$\Delta A = \frac{\Delta A_{\text{max}} \times [S]}{K_d + [S]}$$

where ΔA is the peak-to-trough absorbance difference, ΔA_{max} is the maximum absorbance difference and $[S]$ is the substrate concentration.

NADH turnover assays were performed with mixtures (1.2 mL) containing 50 mM Tris, pH 7.4, 0.5 μM CYP101B1, 5 μM Arx, 0.5 μM ArR and 100 $\mu\text{g mL}^{-1}$ bovine liver catalase. The buffer component was oxygenated by bubbling oxygen through the solution before addition of the other components and equilibration at 30 °C for 2 min. NADH was added to $\sim 320 \mu\text{M}$, final $A_{340} = 2.00$, and the absorbance at 340 nm was monitored. Substrates were added from a 100 mM stock solutions in ethanol or DMSO to a final concentration of 0.25–0.5 mM. The rate of NADH turnover was calculated using $\epsilon_{340} = 6.22 \text{ mM}^{-1} \text{ cm}^{-1}$ (Table 1). Where required turnovers using 4 mM NADH were undertaken in order to generate sufficient product for GC coelution experiments (the rate of NADH oxidation was not monitored).

Table 1 Substrate binding and turnover data for CYP101B1 with naphthalene, biphenyl, naphthols and phenylphenols. The NADH oxidation frequencies were measured using a ArR:Arx:CYP101B1 concentration ratio of 1:10:1 (0.5 μM CYP enzyme, 50 mM Tris, pH 7.4). Rates are reported as mean \pm S.D. ($n \geq 3$) and given in nmol nmol P450 $^{-1}$ min $^{-1a}$

CYP101B1/substrate	% HS heme	NADH oxidation rate ^a (min ⁻¹)
Naphthalene	15%	$\sim 90 \pm 25^b$
1-Naphthol	65%	2090 ± 90
2-Naphthol	40%	560 ± 60
Biphenyl	15%	200 ± 10
2-Phenylphenol	35%	90 ± 1
3-Phenylphenol	40%	80 ± 8
4-Phenylphenol	40%	110 ± 10

^a The NADH oxidation rate is the frequency of NADH oxidation, including product formation and uncoupling reactions. Note for ease of comparison the NADH oxidation rates provided in the main text in the absence of the CYP101B1 enzyme are given in the same units as if the P450 enzyme was present. ^b An estimate of the initial rate of NADH oxidation as the rate increased over time (Fig. 2).

The concentration of hydrogen peroxide formed during NADH oxidation in the absence of CYP101B1 was determined by the horseradish peroxidase/phenol/4-aminoantipyrine assay.⁴⁵ The total assay volume was 800 μL and contained 200 μL of 50 mM Tris, pH 7.4, 400 μL of a reaction mixture, 200 μL of 50 mM phenol and 200 μL of 5 mM 4-aminoantipyrine (both in 50 mM Tris pH 7.4). The absorbance at 510 nm was set to zero, 1 μL of a 20 mg mL $^{-1}$ solution of horseradish peroxidase in water was then added, and the absorbance recorded ($\epsilon_{510} = 6580 \text{ M}^{-1} \text{ cm}^{-1}$).

Product formation

Where authentic product standards were available they were utilised for identification purposes *via* HPLC/GC-MS coelution experiments. The product concentration in the incubation mixtures was calculated by calibrating the UV detector response of the HPLC detector or GC-MS to the total ion count (TIC) to the products. The coupling efficiency was the percentage of NADH consumed that led to product formation. HPLC analyses were performed using an Agilent 1260 Infinity pump equipped with an Agilent Eclipse Plus C18 column (250 mm \times 4.6 mm, 5 μm), an autoinjector and UV detector (monitored at 280 nm for naphthalene turnovers and 254 nm for biphenyl and diclofenac assays). A gradient, 20–95%, of acetonitrile (with trifluoroacetic acid, 0.1%) in water (TFA, 0.1%) was used. The HPLC retention times were as follows; 1-methylnaphthalene, 22.4 min; 1-naphthylmethanol, 15.1 min; 2-methylnaphthalene, 22.4 min; 2-naphthylmethanol, 15.3 min; 2,7-dimethylnaphthalene, 24.4 min; 2-(7-methylnaphthyl)methanol, 17.0 min; 7-methyl-2-naphthoic acid, 17.6 min; 1-ethylnaphthalene, 23.7 min; 1-naphthyl-1-ethanol, 16.6 min; 2-ethylnaphthalene, 24.1 min; 2-naphthyl-1-ethanol, 16.5 min; 2-methylbiphenyl, 23.7 min; 2-biphenylmethanol, 17.4 min; 3-methylbiphenyl, 23.7 min; 3-biphenylmethanol, 17.2 min; 4-methylbiphenyl, 23.7 min; 4-biphenylmethanol, 17.1 min; 4-(4-methylphenyl)phenol, 19.2 min; 4-(4-hydroxyphenyl)benzyl alcohol, 13.0 min; diclofenac, 20.0 min and 4'-hydroxydiclofenac, 16.7 min. The internal standard retention times were 9-fluorenone, 16.6 min and 4-methoxycinnamic acid, 12.6 min.

Gas chromatography-mass spectrometry (GC-MS) analyses were carried out on a Shimadzu GC-17A instrument coupled to a QP5050A MS detector using a Zebron DB-5 MS fused silica column (Phenomenex; 30 m \times 0.25 mm, 0.25 μm) and helium as the carrier gas. The retention times were as follows 1-naphthol 11.0 min; 1,4-naphthoquinone, 9.8 min; 2,6-dihydroxynaphthalene, 14.7 min; 2-naphthol, 11.2 min; biphenyl, 9.6 min; 2-phenylphenol, 11.1 min; 4-phenylphenol, 13.2 min; 3-methylbiphenyl, 10.8 min; 3-phenylbenzaldehyde, 13.0 min; 3-biphenylmethanol, 13.8 min; 4-methylbiphenyl, 10.9 min; 4-biphenylmethanol, 13.9 min and 4-(4-methylphenyl)phenol, 14.3 min. Chiral and additional GC analysis was performed on a Shimadzu Tracer GC coupled to Barrier discharge Ionization Detector (BID) detector using a RT@-BDEXse chiral silica column (Restek; 30 m \times 0.32 mm \times 0.25

um) or a SH-Rxi-5 ms fused silica column (Shimadzu, 30 m × 0.25 mm, 0.25 μm) and helium as the carrier gas. Retention times are given in the ESI† (Fig. S2).

Product isolation and characterisation

To isolate and identify products where standards were not available a whole-cell system utilising the plasmids pETDuetArx/ArR and pRSFDuetArx/CYP101B1 was used to oxidise substrates. These were grown in LB broth, the cells were harvested by centrifugation and resuspended in *E. coli* minimal media (EMM; K₂HPO₄ 7 g, KH₂PO₄ 3 g, Na₃ (citrate) 0.5 g, (NH₄)₂SO₄ 1 g, MgSO₄ 0.1 g, 20% glucose (20 mL), and glycerol (1% v/v) per liter) as described previously.^{27,37} Two aliquots of 0.5 mM substrate were added, one at the beginning of the turnover and the second after 6 h.^{27,37} The supernatant (200 mL) was extracted in ethyl acetate (3 × 100 mL), washed with brine (100 mL) and dried with magnesium sulfate. The organic extracts were pooled and the solvent was removed by vacuum distillation and then under a stream of nitrogen. The products were purified using silica gel chromatography using a hexane/ethyl acetate stepwise gradient ranging from 80:20 to 50:50 hexane to ethyl acetate using 2.5% increases every 100 mL. The composition of the fractions was assessed by TLC and GC-MS and those containing single products (≥95%) were combined for characterisation. The solvent was removed under reduced pressure.

The purified products (ranging from ~3–15 mg) were dissolved in CDCl₃ or d₆-acetone and the organics characterised by NMR spectroscopy. NMR spectra were acquired on an Agilent DD2 spectrometer operating at 500 MHz for ¹H and 126 MHz for ¹³C or a Varian Inova-600 spectrometer operating at 600 MHz for ¹H and 151 MHz for ¹³C. A combination of ¹H, ¹³C, COSY and HSQC experiments were used to determine the structures of the products. Assignments of minor products were made *via* GC coelution or comparison of MS spectra of standards published by others (Fig. S5†).

NMR data

Data for 2-(7-methylnaphthyl)methanol. ¹H NMR (500 MHz, d₆-acetone) δ 7.79 (s, 1H), 7.77 (m, 1H), 7.75 (m, 1H), 7.63 (s, 1H), 7.46 (m, 1H), 7.33 (m, 1H), 4.77 (s, 2H), 2.48 (s, 3H).

Data for 7-methyl-2-naphthoic acid. ¹H NMR (500 MHz, d₆-acetone) δ 8.64 (s, 1H), 8.07 (m, 1H), 8.02 (m, 1H), 7.93 (m, 1H), 7.80 (s, 1H), 7.50 (m, 1H), 2.57 (s, 3H). ¹³C NMR (126 MHz, d₆-acetone) δ 168.38 (C11), 139.78 (C9), 137.26 (C10), 132.31 (C7), 132.06 (C1), 130.52 (C5), 130.36 (C6), 128.85 (C4), 128.51 (C2), 128.09 (C8), 126.83 (C3), 22.35 (C12).

Data for 3-biphenylmethanol. ¹H NMR (500 MHz, CDCl₃) δ 7.64–7.57 (m, 3H), 7.53 (m, 1H), 7.64–7.57 (m, 3H), 7.39–7.31 (m, 2H), 4.77 (s, 2H).

Data for 4'-(4-methylphenyl)phenol. ¹H NMR (500 MHz, CDCl₃) δ 7.45 (m, 2H), 7.43 (m, 2H), 7.22 (m, 2H), 6.88 (m, 2H), 2.38 (s, 3H).

Data for 4'-(4-hydroxyphenyl)benzyl alcohol. ¹H NMR (500 MHz, d₆-acetone) δ 7.54 (m, 2H), 7.50 (m, 2H), 7.40 (m, 2H), 6.92 (m, 2H), 4.65 (s, 2H).

Data for 4'-hydroxydiclofenac^{46,47}. ¹H NMR (600 MHz, d₆-DMSO) δ 7.10 (m, 1H, H4), 7.00–6.96 (m, 1H, H6), 6.93 (s, 2H, 2 × H3'), 6.71 (m, 1H, H5), 6.10 (m, 1H, H7), 3.60 (s, 2H, H2). ¹³C NMR (151 MHz, d₆-DMSO) δ 176.84 (C1), 155.67 (C4'), 144.68 (C8), 133.08 (C1'), 131.04 (C4), 128.63 (C2'), 127.66 (C6), 123.59 (C3), 119.31 (C5), 116.26 (C3'), 113.97 (C7), 35.98 (C2).

Results and discussion

The oxidation of naphthalene and biphenyl by CYP101B1

To investigate the ability of CYP101B1 to oxidise aromatic compounds we analysed naphthalene and biphenyl, each of which contain two aromatic benzene rings (Fig. 1). Substrate binding and enzyme turnover activity were measured using *in vitro* assays. Neither biphenyl nor naphthalene induced a large type I spin-state shift on binding to CYP101B1, both ≤20% high spin (HS) (Table 1, Fig. S1†). The low solubility and relatively weak binding precluded the accurate determination of the dissociation constant for both of these substrates.

Despite this, the addition of naphthalene and biphenyl enhanced the rate of NADH oxidation of the ArR/Arx/CYP101B1 system above the leak rate (the rate of NADH oxidation in the absence of substrate, Table 1). The NADH oxidation activity of the CYP101B1 system with naphthalene was unusual in that it accelerated from an initial rate of 90 nmol nmol P450⁻¹ min⁻¹ (henceforth abbreviated to min⁻¹) over the course of the reaction (Fig. 2a). HPLC and GC-MS analysis of the turnovers revealed minimal levels of the expected naphthol products or any others (Fig. S2†). Therefore it appears that the coupling efficiency, which is the productive use of the NADH reducing equivalents, of naphthalene oxidation by CYP101B1 must be very low. *In vitro* turnovers conducted with a large excess of NADH (4 mM, twelve times the amount in the

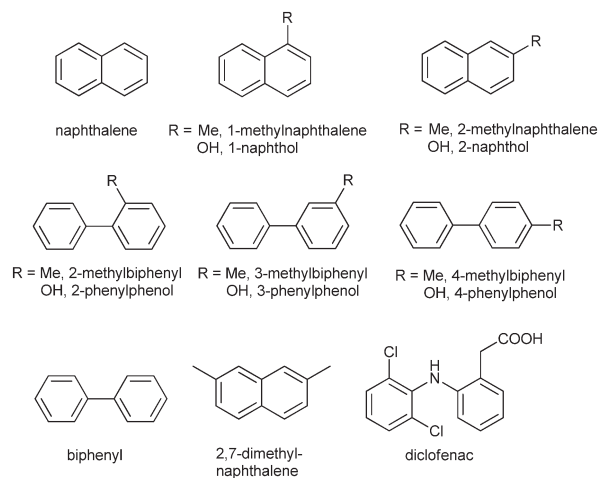


Fig. 1 Substrates tested with CYP101B1.

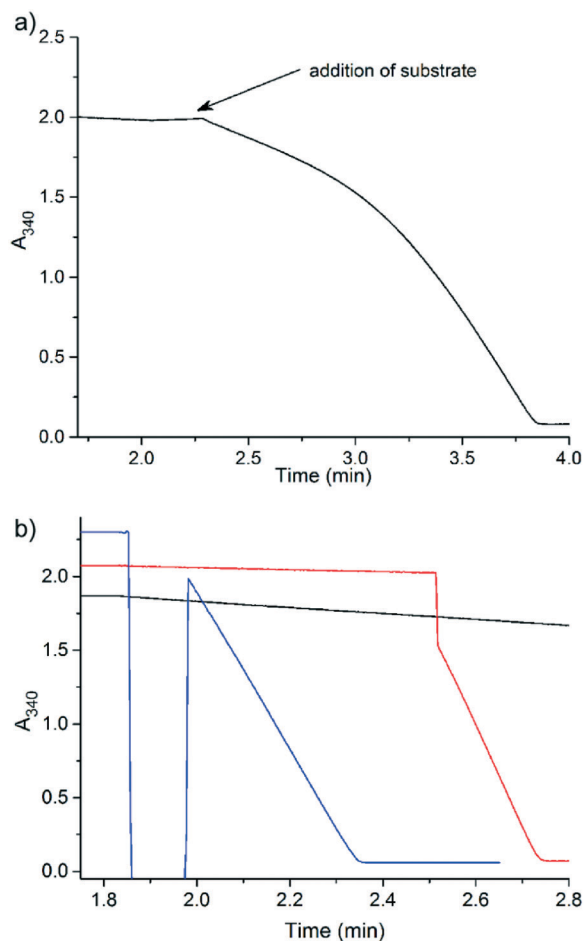
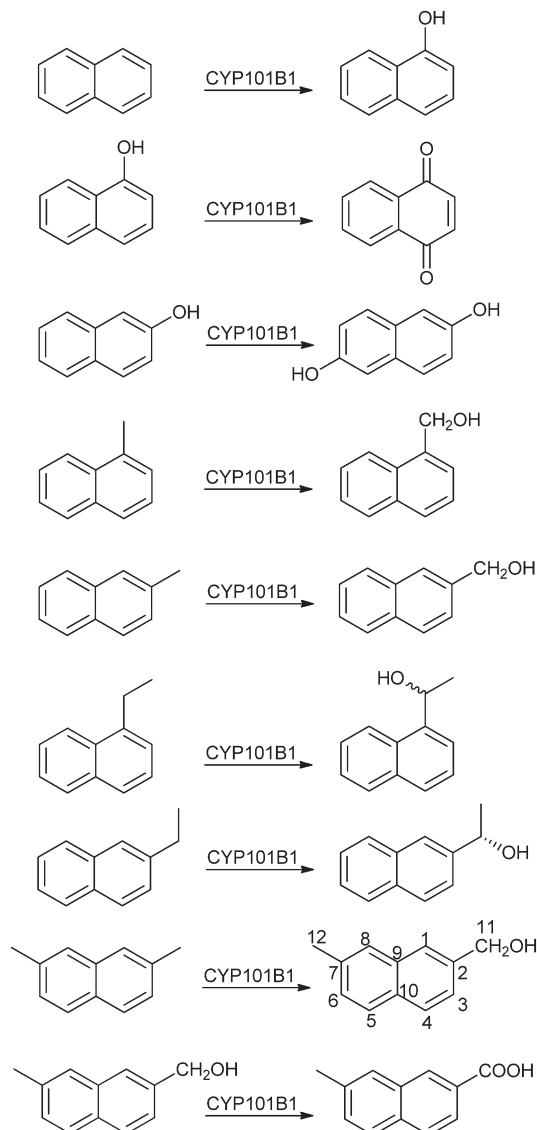


Fig. 2 NADH oxidation assays of CYP101B1 with (a) naphthalene and (b) 1-naphthol (red), 1-naphthol no P450 control (blue) and 1-naphthol, no Arx and P450 control (black).

normal turnover assays) allowed the identification of low levels of 1-naphthol as a product from the CYP101B1 catalysed turnover of naphthalene (Scheme 1, Fig. S2a[†]). Under these conditions biphenyl was oxidised to 4-phenylphenol but the level of product formation was also very low (Fig. S2b[†]).

To investigate if the increasing NADH oxidation rate observed in the CYP101B1 turnovers of naphthalene arose from further oxidation of naphthol products, and to determine if we could identify any product arising from such activity, we tested 1- and 2-naphthol as substrates. 1-Naphthol induced a larger spin state shift (65%, HS, K_d 165 μM) on binding to CYP101B1 than naphthalene, and that induced by 2-naphthol (40%, HS, K_d 195 μM) lay in between (Table 1, Fig. S1 and S3[†]). The NADH oxidation activity of both naphthols was significantly greater than naphthalene. That of 1-naphthol (2090 min^{-1}) being almost 4-fold more active than 2-naphthol (560 min^{-1} , Table S1 and Fig. S4[†]). Analysis of the standard *in vitro* assays was inconclusive for product formation with naphthol substrates due to the low level of metabolites generated. Using excess NADH (4 mM) we were able to detect low levels of product from the oxidation of 1- and 2-naphthol (Fig. S2c and d[†]). 2-Naphthol oxidation resulted in a single



Scheme 1 The products identified from the CYP101B1 turnovers of the naphthalene substrates.

metabolite which was assigned as 2,6-dihydroxynaphthalene by GC coelution experiments with an authentic product standard and analysis of the mass spectrum (Fig. S5[†]).⁴⁸ There was no evidence of either 2-naphthol or the further oxidation product, 2,6-dihydroxynaphthalene, in the CYP101B1 turnovers of naphthalene (Scheme 1, Fig. S2[†]). The product from 1-naphthol oxidation was assigned as 1,4-naphthoquinone based on GC coelution and the mass spectrum (Fig. S2c[†]).^{48,49} A small peak, which coeluted with the 1,4-naphthoquinone, was observed in the turnovers of naphthalene and was also present in the 1-naphthol standard as an impurity (Fig. S2a[†]).

Importantly the quantities of naphthalene and naphthol remaining in these turnovers when excess NADH was used were also high. Further oxidation products, such as those arising from oxidative aryl coupling also do not appear significant.^{31,50,51} This and the low levels of product formation in

the above assays indicated that further oxidation of 1-naphthol or 2-naphthol is unlikely to be the major reason for oxidation of NADH resulting in the acceleration in the activity observed in the naphthalene turnovers (Scheme 1, Fig. S2a†). Control experiments were performed in which the CYP101B1 enzyme was omitted from the turnover. The rate of NADH oxidation in the presence of just the ArR and Arx electron transfer proteins with 1-naphthol (1 mM) was 1560 min^{-1} (Fig. 2). The rate of NADH oxidation in the presence of 2-naphthol in these control reactions, was lower but was similar to that observed in the fully reconstituted *in vitro* turnover (Table 1). When both Arx and CYP101B1 were absent the rate of NADH oxidation dropped dramatically and was similar to the leak rate in the absence of substrate (Fig. 2). We also tested 1,4-naphthoquinone with the Arx and ArR electron transfer partners. The addition of 1,4-naphthoquinone resulted in the rapid oxidation of NADH even at concentrations as low as $8 \mu\text{M}$ ($\sim 2600 \text{ min}^{-1}$) with lower concentrations resulting in significant activity ($4 \mu\text{M}$, 1300 min^{-1} , 50 nM ; 320 min^{-1}). Analysis of these naphthol and naphthoquinone turnovers in the absence and presence of CYP101B1 showed that the majority, $>95\%$, of the reducing equivalents ended up as hydrogen peroxide.

Similar experiments were performed with the three possible phenylphenol products of biphenyl oxidation. The addition of polyphenols to CYP101B1 shifted the spin state to a greater degree than biphenyl (35–40%, Table 1) but the NADH oxidation activities were all lower than that of biphenyl and much lower than those of the naphthols ($\leq 110 \text{ min}^{-1}$, Table 1). The NADH oxidation rate in the absence of CYP101B1 was also similar to those of the phenylphenols in the normal turnover assays but the levels of hydrogen peroxide generated were low for 2- and 4-phenylphenol ($< 10 \mu\text{M}$). The levels were slightly higher for 3-phenylphenol ($\sim 20 \mu\text{M}$).

The data suggests that the unusual behavior of naphthalene oxidation by the ArR/Arx/CYP101B1 system is predominantly due to an increase in the NADH oxidation activity of the system in the presence of small quantities of 1,4-naphthoquinone. This arises from hydroxylation of naphthalene to 1-naphthol followed by further oxidation to the quinone. The increased rate observed with 1-naphthol is most likely due to low levels of a quinone impurity. Rather than 1,4-naphthoquinone acting as a substrate or promoting established P450 uncoupling pathways it accepts electrons from Arx and in the aerobic environment of the turnover was able to reduce oxygen. Oxygen is likely to be reduced to superoxide which dismutates to hydrogen peroxide and singlet oxygen. This would be similar to reactivity reported for NADPH cytochrome P450 reductase (FAD/FMN cofactors) with quinones and nitroaromatics and that observed with the leaking of reducing equivalent in the adrenodoxin mitochondrial system.^{52–54} The reduction of oxygen by the mitochondrial electron transfer system in the absence of substrate and the P450 enzyme has been described before.^{54,55} The acceleration of this uncoupling pathway by exogenous substrates has not been described in great detail with bacterial or mito-

chondrial electron transfer systems containing ferredoxins.^{5,12,56–58} This redox cycling competes with electron transfer to CYP101B1 and therefore reduces the levels of metabolite formation. This resulted in low levels of productive P450 catalysis despite high levels of NADH oxidation activity and should be considered an additional form of uncoupling in P450 systems. Further investigations are required to determine the exact mechanism of the transfer of the electrons from the ferredoxin to the naphthoquinone and the subsequent generation of hydrogen peroxide. It would also be important to ascertain if this behaviour is generic across the class I electron transfer systems and to understand the structural features of the molecules which can interfere with the electron transfer process in this way.^{57,58} The increase in the rate of futile redox cycling during the turnovers was greatest for the oxidation products arising from naphthalene oxidation to 1-naphthol and 1,4-naphthoquinone with minimal activity of this type being observed with phenylphenols, biphenylmethanols or naphthylmethanols (*vide infra*). We note that the 1,4-naphthoquinone and 2,6-dihydroxynaphthalene metabolites which arose from the turnovers of the naphthols are the same as those observed in the metabolism of these substrates by mammalian P450 enzymes.^{59,60} This phenomenon is likely to have important implications for understanding the toxicity of polyaromatic hydrocarbons and their oxygenated metabolites such as quinones.^{61,62}

Oxidation of substituted two ring aromatic molecules by CYP101B1

The low productive monooxygenase activity of CYP101B1 with naphthalene and biphenyl, led us to investigate similar substrates which contain more reactive benzylic aliphatic C–H bonds (Fig. 1). 1-Methylnaphthalene bound to CYP101B1, with a spin state shift of 55% HS (Fig. S1†) which is greater than naphthalene and almost as high as 1-naphthol. We were able to measure the dissociation constant of 1-methylnaphthalene binding to CYP101B1, K_d $63 \mu\text{M}$ (Fig. 3).

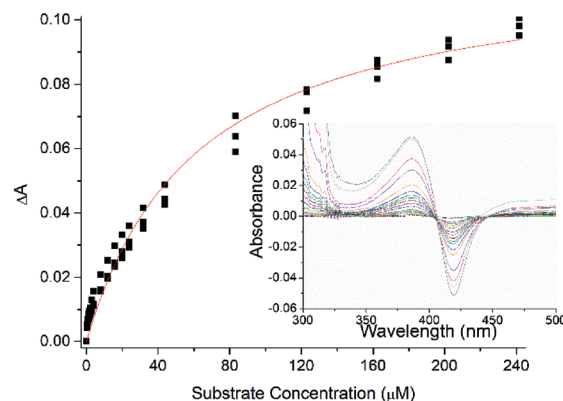


Fig. 3 Dissociation constant analysis of CYP101B1 with 1-methylnaphthalene ($2.1 \mu\text{M}$ enzyme/ K_d $63 \pm 5 \mu\text{M}$, peak to trough, $A_{390} - A_{420}$).

This was weaker than that of norisoprenoids, monoterpene acetates and phenylcyclohexane but tighter than most monoterpeneoids.⁴¹ The NADH oxidation activity (240 min^{-1}) was higher than the initial rate observed with naphthalene and it was linear throughout the turnover (Table 2, Fig. S4†). HPLC analysis revealed the formation of a single product, which coeluted with an authentic standard of 1-naphthylmethanol (Scheme 1 and Fig. 4). The amount of 1-naphthylmethanol was quantitated and both the product formation rate, 38 min^{-1} , and coupling efficiency, 16%, for the turnovers were determined.

2-Methylnaphthalene induced a smaller spin state shift with a lower binding affinity, 40% HS and K_d 135 μM , compared to 1-methylnaphthalene (Fig. S1 and S3†). The NADH oxidation activity of CYP101B1 in the presence of 2-methylnaphthalene was 212 min^{-1} . A single product, 2-naphthylmethanol, identified by HPLC coelution, was formed at a product formation rate of 57 min^{-1} (Scheme 1 and Fig. 4). The higher activity of 2-methylnaphthalene oxidation compared to 1-methylnaphthalene arose as a result of greater coupling efficiency of the reducing equivalents to product formation, 26% (Table 2).

The effect of the size of the alkyl substituent on the binding and biocatalytic parameters of CYP101B1 was investigated by testing 1- and 2-ethylnaphthalene. Addition of both substrates induced spin state shifts of only 20% HS, which was lower than the equivalent methylnaphthalenes but comparable to naphthalene. The dissociation constants indicated that binding was tighter than the methylnaphthalenes (Table 2, Fig. S3†). The NADH oxidation activity of CYP101B1 with 1-ethylnaphthalene (482 min^{-1}) was greater than that of 2-ethylnaphthalene (284 min^{-1}) and both methylnaphthalenes (Table 2). A single product was generated from each of the turnovers of 1- and 2-ethylnaphthalene. These coeluted with 1-naphthyl-1-ethanol and 2-naphthyl-1-ethanol, respectively (Scheme 1, Fig. 4 and Fig. S6†). The product formation rate with 1-ethylnaphthalene (18 min^{-1}) was lower than 2-ethylnaphthalene (20 min^{-1}). Despite the higher NADH oxidation rates and the greater reactivity of the benzylic methylene group of these substrates, *versus* the methyl group of the

methylnaphthalenes, the coupling of reducing equivalents to product formation decreased (both $<10\%$, Table 2). The lower coupling efficiencies and product formation rates observed for both of these substrates compared to the methylnaphthalenes is consistent with the reduced spin state shifts observed on substrate binding.

Chiral GC analysis showed that the turnover of 2-ethylnaphthalene generated a single enantiomer which coeluted with (*R*)-(+)-1-(2-naphthyl)ethanol (Fig. S2(e)†). The enantioselectivity of 1-ethylnaphthalene oxidation was lower with both enantiomers of 1-naphthyl-1-ethanol were generated though there was a significant excess of one stereoisomer ($\sim 84\%$ ee, Fig. S2(f)†). Overall the larger ethyl naphthalenes bind tightly but do not appear to be positioned as well in the active site of CYP101B1 for efficient C–H bond oxidation when compared to the methyl naphthalenes. However they must be positioned in such a way that there is a strong preference for abstraction of one of the enantiotopic hydrogens of the methylene group.

2,7-Dimethylnaphthalene induced a lesser spin state shift on binding to CYP101B1, 30% HS, than either 1- or 2-methylnaphthalene. However the binding affinity of this substrate was higher than any other tested (K_d 14 μM , Table 2). The activity of CYP101B1 with 2,7-dimethylnaphthalene was high as measured by NADH oxidation (448 min^{-1} , Table 1). The product formation rate was the greatest of all the substituted naphthalenes (79 min^{-1}) and the coupling efficiency (18%) was comparable to that of the methylnaphthalenes. The *in vitro* turnover produced a single oxidation product (Fig. 4d). The most likely product, which could arise from benzylic C–H bond hydroxylation of 2,7-dimethylnaphthalene, was not available for coelution so a whole-cell oxidation turnover was conducted to generate metabolites for characterisation. The *in vivo* turnover converted all the added substrate (1 mM, Fig. 4d) into a single oxidation product after 20 hours. The metabolite from the whole-cell oxidation was isolated and identified by NMR as 7-methyl-2-naphthoic acid. The characteristic signal was the chemical shift of 168.38 ppm in the ^{13}C NMR, corresponding to a carboxylic acid, and this combined with the lack of

Table 2 Substrate binding, turnover and coupling efficiency data for the turnovers of CYP101B1 with alkyl substituted naphthalene and biphenyl substrates. The turnover activities were measured using a ArR:Arx:CYP101B1 concentration ratio of 1:10:1 (0.5 μM CYP enzyme, 50 mM Tris, pH 7.4). *N* is the NADH oxidation rate (as defined in Table 1), PFR the product formation rate and *C* is the coupling efficiency, which is the percentage of NADH utilised for the formation of products. Rates are reported as mean \pm S.D. ($n \geq 3$) and given in $\text{nmol nmol}_{\text{CYP}}^{-1} \text{min}^{-1}$

CYP101B1/substrate	% HS	K_d^a (μM)	<i>N</i>	PFR	<i>C</i> %
1-Methylnaphthalene	55%	63	240 ± 17	38 ± 10	16
2-Methylnaphthalene	40%	135	212 ± 24	57 ± 18	26
2,7-Dimethylnaphthalene	30%	14	448 ± 44	79 ± 10	18
1-Ethylnaphthalene	20%	40	482 ± 7	18 ± 3	4
2-Ethylnaphthalene	20%	45	284 ± 5	20 ± 1	7
2-Methylbiphenyl	20%	29	257 ± 9	35 ± 8	14
3-Methylbiphenyl	20%	17	127 ± 10	30 ± 12	23
4-Methylbiphenyl	20%	30	176 ± 10	39 ± 7	22
4-Biphenylmethanol	10%	—	106 ± 8	11 ± 4	12

^a See Fig. S3 for details.

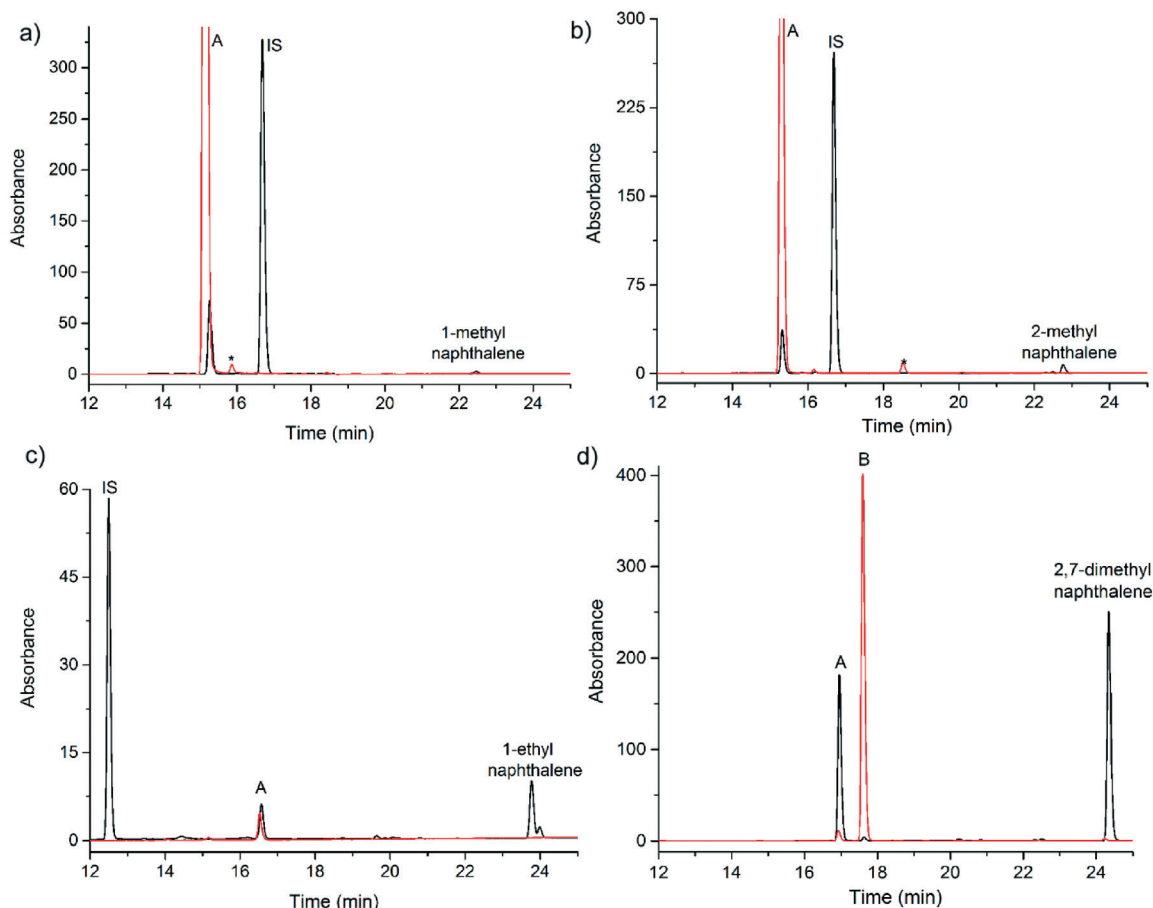
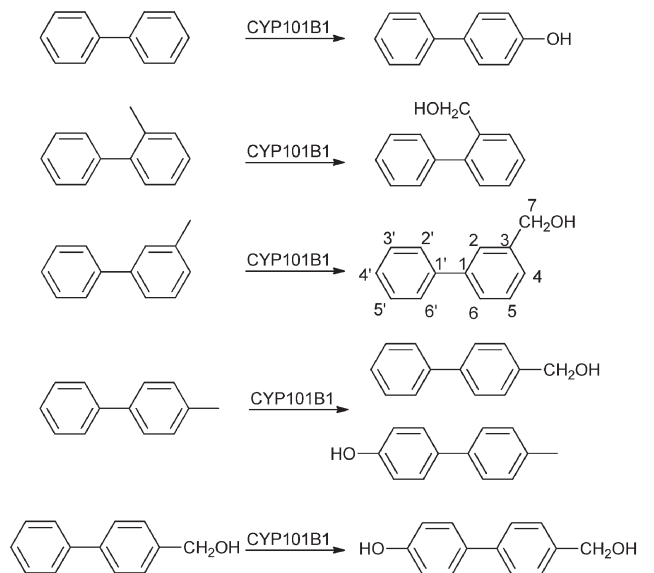


Fig. 4 HPLC analysis of the *in vitro* CYP101B1 turnovers of (a) 1-methylnaphthalene overlaid with 1-naphthylmethanol, (b) 2-methylnaphthalene overlaid with 2-naphthylmethanol, (c) 1-ethylnaphthalene overlaid with 1-naphthyl-1-ethanol and (d) 2,7-dimethylnaphthalene overlaid with the whole-cell oxidation turnover of the same substrate. Turnovers are shown in black the internal standard (IS), impurities (*) and substrate are labelled. The HPLC runs of the authentic product standards (A) are shown in red for (a–c). In (d) the whole-cell product turnover which generated 7-methyl-2-naphthoic acid (B) is in red. A different internal standard, 4-methoxycinnamic acid, was used in the turnover of 1-ethylnaphthalene as 9-fluorenone coeluted with the 1-naphthyl-1-ethanol product.

CH₂OH peak and presence of all six aromatic protons in ¹H NMR allowed identification (Fig. S7†). However this naphthoic acid metabolite did not coelute with the product from the *in vitro* enzyme turnovers. 7-Methyl-2-naphthoic acid was reduced using an excess of lithium aluminium hydride and the single product generated was found to coelute with that obtained in the enzyme turnover assays. NMR analysis of this product confirmed it was the expected metabolite, 2-(7-methylnaphthyl)methanol (Fig. S8†). In the *in vitro* turnover the limiting amount of NADH compared to substrate, precludes the further oxidation of 2-(7-methylnaphthyl)methanol but in the whole-cell oxidation system all of the substrate was converted to the alcohol product, which is then further oxidised to the carboxylic acid (Scheme 1). Presumably this occurs *via* the aldehyde, though this intermediate product was not observed in either the *in vivo* or *in vitro* turnovers. The total conversion of 1 mM substrate into the carboxylic acid in the whole-cell oxidations corresponds to approximately 4500 turnovers based on an enzyme concentration of 0.65 μM.³⁷

Methylbiphenyls with the substituent at the 2-, 3- and 4-positions were also investigated (Fig. 1). All three compounds induced a small shift to the high spin state upon binding to CYP101B1 (~20%, HS, Fig. S1†). This was greater than biphenyl but lower than the equivalent phenylphenols (Table 1). The binding affinities were higher than the mono-substituted naphthalenes with that of 3-methylbiphenyl approaching that of 2,7-dimethylnaphthalene (Table 2, Fig. S3†).

The NADH oxidation activity of CYP101B1 after addition of the methylbiphenyls was similar to that of biphenyl but faster than all the phenylphenols (Table 1) and varied as follows; 2-methylbiphenyl > 1-methylnaphthalene > 2-methylnaphthalene > 4-methylbiphenyl > 3-methylbiphenyl. That of 3-methylbiphenyl (127 min⁻¹) was approximately half that of 2-methylbiphenyl (257 min⁻¹, Table 2). Overall the product formation activity of 2-methylbiphenyl and 3-methylbiphenyl were similar (30 to 35 min⁻¹; Table 2). The *in vitro* turnovers of 2- and 3-methylbiphenyl generated 2- and 3-biphenylmethanol, respectively, as the sole products



Scheme 2 The products formed from the CYP101B1 catalysed oxidation of biphenyl substrates.

(Scheme 2 and Fig. 5). 2-Biphenylmethanol was identified by HPLC coelution experiments with an authentic product standard (Fig. 5a). 3-Biphenylmethanol was generated using the whole-cell oxidation system, purified by silica chromatography and identified by NMR, the 2H signal at 4.77 ppm and the signals of nine hydrogens in the aromatic region allowed characterisation (Fig. S9[†]). There was no evidence of further oxidation of either product when using the whole-cell oxidation system, despite only a small amount of 3-methylbiphenyl substrate remaining. Low levels of 3-phenylbenzaldehyde were detected by GC-MS analysis of the *in vitro* turnovers of 3-methylbiphenyl when excess NADH (4 mM) was used (Fig. S5[†]).

The turnover of 4-methylbiphenyl was more complex and resulted in the formation of two metabolites. The product formation rate of the 4-methylbiphenyl (39 min^{-1}) and the efficiency (22%) resembled those of 2- and 3-methylbiphenyl despite the different P450 mechanisms involved in aromatic *versus* aliphatic oxidation.⁶³ The minor product 4-biphenylmethanol (30%) was identified *via* HPLC coelution with an authentic product standard (Fig. 5c). As with 2,7-dimethylnaphthalene we considered that the major product

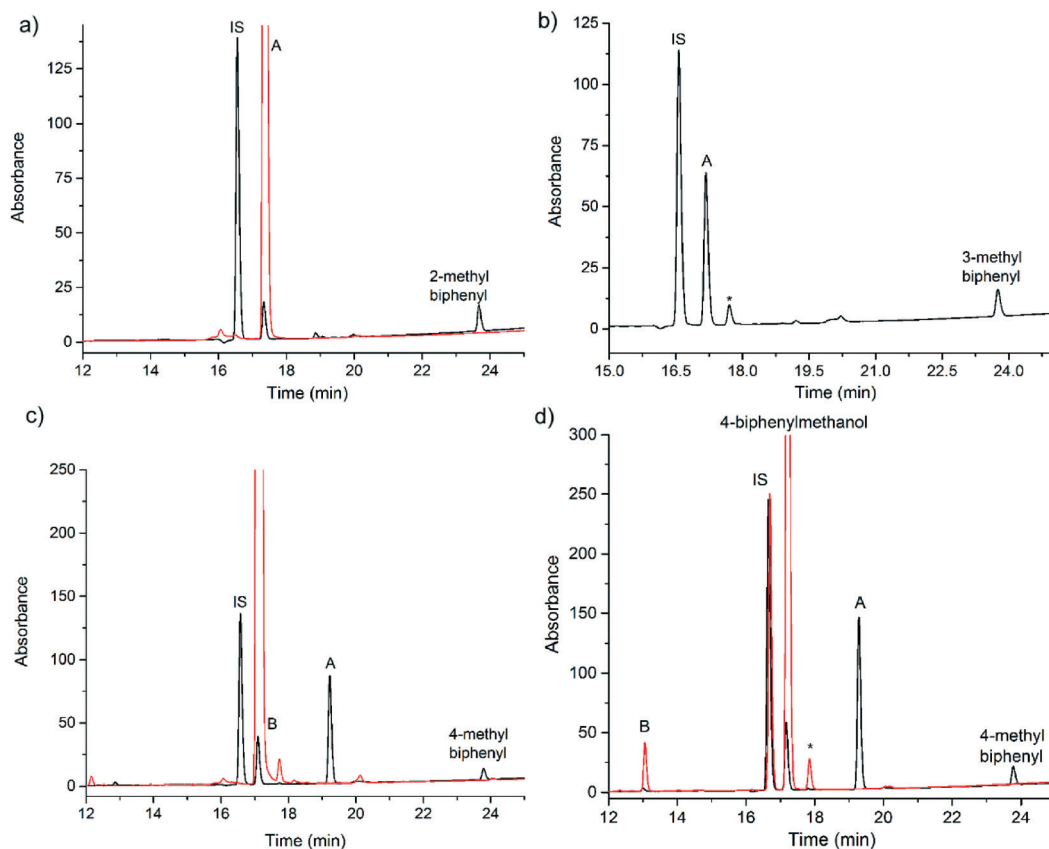


Fig. 5 HPLC analysis of the *in vitro* CYP101B1 turnovers of (a) 2-methylbiphenyl overlaid with 2-biphenylmethanol, (b) 3-methylbiphenyl, (c) 4-methylbiphenyl overlaid with 4-biphenylmethanol and (d) 4-methylbiphenyl overlaid with the turnover of 4-biphenylmethanol. Turnovers are shown in black the internal standard (IS), impurities (*) and substrate are labelled. The HPLC chromatograms of the authentic product standards (A) are shown in red for (a) and (b). In (c) and (d) the peak labelled A is the 4'-(4-methylphenyl)phenol major product. In (c) the peak labelled B is 4-biphenylmethanol and in (d) it is 4'-(4-hydroxyphenyl)benzyl alcohol.

(70%) may arise from further oxidation of the 4-biphenylmethanol product generating the aldehyde or the carboxylic acid. Whole-cell oxidation turnovers were conducted with 4-biphenylmethanol and 4-methylbiphenyl. The product from the oxidation of 4-biphenylmethanol did not coelute with any peaks in the 4-methylbiphenyl turnover (Fig. 5d). Therefore the unidentified product from the whole-cell turnover of 4-methylbiphenyl was isolated by silica column chromatography and characterised. The 3H methyl singlet (2.38 ppm) and the distinctive signals of the two *para*-substituted rings (8H) in the aromatic region allowed identification as 4'-(4-methylphenyl)phenol (Scheme 2, Fig. S10†).

The product of CYP101B1 catalysed oxidation of 4-biphenylmethanol was also isolated and characterised by NMR as 4'-(4-hydroxyphenyl)benzyl alcohol (Fig. S11†). The NADH oxidation rate, product formation rate and the coupling efficiency of the turnover of 4-biphenylmethanol were also measured and found to be lower than those of the methylbiphenyls (Table 2).

4-Methylbiphenyl is unusual in that the major product arises from oxidation at an aromatic C–H bond with the minor product being hydroxylation at the more reactive benzylic methyl group. In addition, unlike 2,7-dimethylnaphthalene further oxidation to the carboxylic acid is less favoured when compared to aromatic oxidation on the other benzene ring. This substrate must be bound in at least two orientations with the most favourable leading to oxidation of the aromatic C–H bond. In the second orientation the methyl group would be located close enough to the heme iron-oxo intermediate to favour C–H bond abstraction at the sp^3 hydrogens.

The alcohol oxygen of 4-biphenylmethanol, may favour binding of the substrate in an orientation with the *para* aromatic ring closest to the heme iron. This would be in broad agreement with the regioselectivity observed with the oxygen containing norisoprenoids and monoterpenoid acetates. It is of note that 4-methylbiphenyl and 4-biphenylmethanol are the only two substrates tested so far with CYP101B1 where oxidation at an aromatic C–H bond is preferred over aliphatic oxidation. The CYP101B1 catalysed oxidation of phenylcyclohexane, *p*-cymene and the other methyl substituted naphthalenes and biphenyls favoured aliphatic hydroxylation. 4-Methylbiphenyl and 4-biphenylmethanol must have a shape which allows them to bind in a different orientation in the substrate binding pocket of CYP101B1.

The majority of the substrates are presumably held in orientations such that that the initial formation of the arene oxide intermediate in the NIH shift mechanism^{64,65} or Shaik's porphyrin mediated proton-shuttle mechanism,⁶³ required for aromatic oxidation, must be impeded (Scheme S1†). If aromatic oxidation does occur *via* an arene oxide intermediate this pathway could also generate 3-(4-methylphenyl)phenol. This product was not observed, perhaps as it would be formed *via* a less favoured cationic intermediate (Scheme S1†).

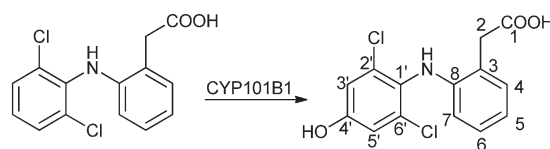
With the exception of 4-methylbiphenyl the alkyl substituted aromatic substrates hydroxylated by CYP101B1 with high regioselectivity for the benzylic C–H bonds of the

methyl or ethyl substituent. This is in accordance with the reactivity of the C–H bonds in these substrates. The preference for aliphatic *versus* aromatic oxidation, may reflect the different mechanisms and energies of aromatic *versus* aliphatic C–H bond oxidation. The size and planar nature of the naphthalene and biphenyl molecules may limit the motion of the substrate in the active site. The alkyl group of the substrates is likely to be held close to the heme in at least one of the preferred binding orientations in order to allow the generation of the observed products.

Finally we used CYP101B1 to oxidise the nonsteroidal anti-inflammatory drug molecule diclofenac. Diclofenac consists of two aromatic rings linked through an amine group (diphenylamine like), and contains a carboxylic acid moiety as well as two chlorines (Fig. 1). The carboxylate group oxygen could potentially mimic the ketone functionality of norisoprenoids, which bind efficiently to CYP101B1. The binding of diclofenac induced a minimal shift in the spin state of CYP101B1, ~5% HS, upon binding. The NADH oxidation rate could not be accurately determined as the substrate absorbs strongly at 340 nm. However HPLC analysis of a whole-cell oxidation turnover of diclofenac indicated that a single product was formed (Fig. S12†). This was generated in larger quantities using the whole-cell oxidation system and purified by silica gel chromatography. The product was identified as 4'-hydroxydiclofenac by matching its NMR data to that reported in the literature (Scheme 3).^{46,47}

As a control we tested diphenylmethane with the CYP101B1 enzyme. This was a poor substrate for CYP101B1 but showed low activity with hydroxylation occurring at the benzylic C–H bonds (Fig. S5 and S13†). The selective oxidation of the drug molecule diclofenac by “wild-type” CYP101B1 is a promising step towards using this system for drug metabolite production from molecules with similar structural features to naphthalene, biphenyl and diclofenac. CYP101B1 could be used to mimic the drug oxidising properties of mammalian P450 enzymes and thus allow the facile generation of hydroxylated drug metabolites in larger quantities.

Previously we have shown that CYP101B1 has a strong preference for substrates containing a carbonyl oxygen group such as norisoprenoids and monoterpenoid esters which presumably arises through some hydrophilic interactions with the residues that line the active site of the enzyme. The binding affinity of the more apolar aromatic substrates tested here could therefore be improved using protein engineering to increase the hydrophobicity of the active site. The size of the substrate binding pocket could also be modified to better



Scheme 3 The product formed from the CYP101B1 turnover with diclofenac. The numbering system used for diclofenac is the same as that from Marco-Urrea *et al.*⁴⁶

accommodate these aromatic molecules. However there is currently no structural information available for the CYP101B1 enzyme. These approaches would lead to significant improvement in the coupling efficiency and product formation rate leading to more efficient biocatalytic oxidation of naphthalene and biphenyl based substrates.

Conclusions

We have shown that CYP101B1 is capable of oxidising a range of molecules containing two aromatic rings. The oxidation of naphthalene and biphenyl were inefficient and one of the products generated during the turnover of naphthalene could compete with CYP101B1 for electrons from the ArR/Arx electron transfer system *via* redox cycling. This form of uncoupling of reducing equivalents would make regular cytochrome P450 enzymes unsuitable biocatalysts for naphthalene oxidation and using alternate systems such as peroxygenases may be more effective. CYP101B1 was able to efficiently and selectively oxidise a range of alkyl substituted naphthalene and biphenyl substrates. The product formation activities are comparable or in excess to other available systems and the selective oxidation and total turnovers achieved using a whole-cell oxidation system with CYP101B1 with these hydrophobic substrates is suited to the biocatalytic generation of hydroxylated products. The reactions are, in general, regioselective for oxidation at the more reactive benzylic carbons. 4-Methylbiphenyl was the exception being preferably oxidised to 4'-(4-methylphenyl)phenol with 4-biphenylmethanol being formed as a minor product. The oxidation of both ethylnaphthalenes by CYP101B1 was also highly enantioselective. The aromatic drug molecule diclofenac, which also contains two aromatic rings, was regioselectively hydroxylated to 4'-hydroxydiclofenac. When incorporated into a whole-cell oxidation system, with the physiological electron transfer partners, ArR and Arx, CYP101B1 was capable of generating the oxidised metabolites of the substituted naphthalenes and biphenyls in sufficient amounts for characterisation. In certain instances further oxidation products were formed using the whole-cell oxidation system for example 2,7-dimethylnaphthalene oxidation generated the further oxidation product 7-methyl-2-naphthoic acid as the only metabolite.

Acknowledgements

E. A. H. and R. S. thank the University of Adelaide for M. Phil and International PhD Scholarships, respectively. S. G. B. acknowledges the ARC for a Future Fellowship (FT140100355).

References

- R. Bernhardt, *J. Biotechnol.*, 2006, **124**, 128–145.
- C. J. Whitehouse, S. G. Bell and L. L. Wong, *Chem. Soc. Rev.*, 2012, **41**, 1218–1260.
- R. Bernhardt and V. B. Urlacher, *Appl. Microbiol. Biotechnol.*, 2014, **98**, 6185–6203.
- T. Furuya and K. Kino, *Appl. Microbiol. Biotechnol.*, 2010, **86**, 991–1002.
- Cytochrome P450: Structure, Mechanism, and Biochemistry*, ed. P. R. Ortiz de Montellano, Springer International Publishing, Switzerland, 2015.
- The Ubiquitous Roles of Cytochrome P450 Proteins*, ed. A. Sigel, H. Sigel and R. Sigel, John Wiley & Sons, 2007.
- S. G. Bell, N. Hoskins, C. J. C. Whitehouse and L. L. Wong, in *Metal Ions in Life Sciences*, ed. A. Sigel, H. Sigel and R. Sigel, John Wiley & Sons, Chichester, UK, 1st edn, 2007, ch. 14, vol. 3, pp. 437–652.
- F. Hannemann, A. Bichet, K. M. Ewen and R. Bernhardt, *Biochim. Biophys. Acta*, 2007, **1770**, 330–344.
- J. A. Peterson and S. E. Graham-Lorence, in *Cytochrome P450: Structure, Mechanism, and Biochemistry*, ed. P. R. Ortiz de Montellano, Plenum Press, New York, 2nd edn, 1995, pp. 151–182.
- S. G. Bell, F. Xu, E. O. Johnson, I. M. Forward, M. Bartlam, Z. Rao and L. L. Wong, *J. Biol. Inorg. Chem.*, 2010, **15**, 315–328.
- W. Yang, S. G. Bell, H. Wang, W. Zhou, N. Hoskins, A. Dale, M. Bartlam, L. L. Wong and Z. Rao, *J. Biol. Chem.*, 2010, **285**, 27372–27384.
- D. Holtmann and F. Hollmann, *ChemBioChem*, 2016, **17**, 1391–1398.
- P. J. Loida and S. G. Sligar, *Biochemistry*, 1993, **32**, 11530–11538.
- E. J. Mueller, P. J. Loida and S. G. Sligar, in *Cytochrome P450: Structure, Mechanism, and Biochemistry*, ed. P. R. Ortiz de Montellano, Plenum Press, New York, 2nd edn, 1995, pp. 83–124.
- S. G. Bell, X. Chen, R. J. Sowden, F. Xu, J. N. Williams, L. L. Wong and Z. Rao, *J. Am. Chem. Soc.*, 2003, **125**, 705–714.
- G. D. Roiban and M. T. Reetz, *Chem. Commun.*, 2015, **51**, 2208–2224.
- K. Zhang, B. M. Shafer, M. D. Demars 2nd, H. A. Stern and R. Fasan, *J. Am. Chem. Soc.*, 2012, **134**, 18695–18704.
- K. Syed, A. Porollo, Y. W. Lam, P. E. Grimmett and J. S. Yadav, *Appl. Environ. Microbiol.*, 2013, **79**, 2692–2702.
- K. Syed, A. Porollo, Y. W. Lam and J. S. Yadav, *PLoS One*, 2011, **6**, e28286.
- S. G. Bell, W. Yang, J. A. Yorke, W. Zhou, H. Wang, J. Harmer, R. Copley, A. Zhang, R. Zhou, M. Bartlam, Z. Rao and L. L. Wong, *Acta Crystallogr., Sect. D: Biol. Crystallogr.*, 2012, **68**, 277–291.
- M. J. Pecyna, R. Ullrich, B. Bittner, A. Clemens, K. Scheibner, R. Schubert and M. Hofrichter, *Appl. Microbiol. Biotechnol.*, 2009, **84**, 885–897.
- A. B. Carmichael and L.-L. Wong, *Eur. J. Biochem.*, 2001, **268**, 3117–3125.
- A. V. Grinberg, F. Hannemann, B. Schiffler, J. Muller, U. Heinemann and R. Bernhardt, *Proteins*, 2000, **40**, 590–612.
- Y. Hiruma, M. A. Hass, Y. Kikui, W. M. Liu, B. Olmez, S. P. Skinner, A. Blok, A. Kloosterman, H. Koteishi, F. Lohr, H. Schwalbe, M. Nojiri and M. Ubbink, *J. Mol. Biol.*, 2013, **425**, 4353–4365.

- 25 P. A. England, C. F. Harford-Cross, J.-A. Stevenson, D. A. Rouch and L.-L. Wong, *FEBS Lett.*, 1998, **424**, 271–274.
- 26 P. A. England, D. A. Rouch, A. C. G. Westlake, S. G. Bell, D. P. Nickerson, M. Webberley, S. L. Flitsch and L. L. Wong, *Chem. Commun.*, 1996, 357–358.
- 27 S. G. Bell, C. F. Harford-Cross and L.-L. Wong, *Protein Eng.*, 2001, **14**, 797–802.
- 28 C. F. Harford-Cross, A. B. Carmichael, F. K. Allan, P. A. England, D. A. Rouch and L. L. Wong, *Protein Eng.*, 2000, **13**, 121–128.
- 29 S. G. Bell, D. A. Rouch and L.-L. Wong, *J. Mol. Catal. B: Enzym.*, 1997, **3**, 293–302.
- 30 C. Y. Lin, A. M. Wheelock, D. Morin, R. M. Baldwin, M. G. Lee, A. Taff, C. Plopper, A. Buckpitt and A. Rohde, *Toxicology*, 2009, **260**, 16–27.
- 31 N. Misawa, M. Nodate, T. Otomatsu, K. Shimizu, C. Kaido, M. Kikuta, A. Ideno, H. Ikenaga, J. Ogawa, S. Shimizu and K. Shindo, *Appl. Microbiol. Biotechnol.*, 2011, **90**, 147–157.
- 32 T. Makino, T. Otomatsu, K. Shindo, E. Kitamura, G. Sandmann, H. Harada and N. Misawa, *Microb. Cell Fact.*, 2012, **11**, 95.
- 33 G. A. Roberts, G. Grogan, A. Greter, S. L. Flitsch and N. J. Turner, *J. Bacteriol.*, 2002, **184**, 3898–3908.
- 34 E. Aranda, R. Ullrich and M. Hofrichter, *Biodegradation*, 2010, **21**, 267–281.
- 35 J. K. Fredrickson, D. L. Balkwill, G. R. Drake, M. F. Romine, D. B. Ringelberg and D. C. White, *Appl. Environ. Microbiol.*, 1995, **61**, 1917–1922.
- 36 Y. Lyu, W. Zheng, T. Zheng and Y. Tian, *PLoS One*, 2014, **9**, e101438.
- 37 S. G. Bell, A. Dale, N. H. Rees and L. L. Wong, *Appl. Microbiol. Biotechnol.*, 2010, **86**, 163–175.
- 38 W. Yang, S. G. Bell, H. Wang, W. Zhou, M. Bartlam, L. L. Wong and Z. Rao, *Biochem. J.*, 2011, **433**, 85–93.
- 39 M. Ma, S. G. Bell, W. Yang, Y. Hao, N. H. Rees, M. Bartlam, W. Zhou, L. L. Wong and Z. Rao, *ChemBioChem*, 2011, **12**, 88–99.
- 40 S. G. Bell and L. L. Wong, *Biochem. Biophys. Res. Commun.*, 2007, **360**, 666–672.
- 41 E. A. Hall and S. G. Bell, *RSC Adv.*, 2015, **5**, 5762–5773.
- 42 E. A. Hall, M. R. Sarkar, J. H. Z. Lee, S. D. Munday and S. G. Bell, *ACS Catal.*, 2016, **6**, 6306–6317.
- 43 J. E. Stok, E. A. Hall, I. S. J. Stone, M. C. Noble, S. H. Wong, S. G. Bell and J. J. De Voss, *J. Mol. Catal. B: Enzym.*, 2016, **128**, 52–64.
- 44 M. R. Sarkar, E. A. Hall, S. Dasgupta and S. G. Bell, *ChemistrySelect*, 2016, **1**, 6700–6707.
- 45 F. Xu, S. G. Bell, Z. Rao and L. L. Wong, *Protein Eng., Des. Sel.*, 2007, **20**, 473–480.
- 46 E. Marco-Urrea, M. Pérez-Trujillo, C. Cruz-Morató, G. Caminal and T. Vicent, *J. Hazard. Mater.*, 2010, **176**, 836–842.
- 47 S.-H. Kim, J.-H. Kwon and S.-H. Yoon, *Bull. Korean Chem. Soc.*, 2010, **31**, 3007–3009.
- 48 SDBSWeb: <http://sdfs.db.aist.go.jp> (National Institute of Advanced Industrial Science and Technology).
- 49 O. Suchard, R. Kane, B. J. Roe, E. Zimmermann, C. Jung, P. A. Waske, J. Mattay and M. Oelgemöller, *Tetrahedron*, 2006, **62**, 1467–1473.
- 50 E. M. Gillam, L. M. Notley, H. Cai, J. J. De Voss and F. P. Guengerich, *Biochemistry*, 2000, **39**, 13817–13824.
- 51 O. Shoji, C. Wiese, T. Fujishiro, C. Shirataki, B. Wunsch and Y. Watanabe, *J. Biol. Inorg. Chem.*, 2010, **15**, 1109–1115.
- 52 H. Kappus, *Biochem. Pharmacol.*, 1986, **35**, 1–6.
- 53 J. W. Chu and T. Kimura, *J. Biol. Chem.*, 1973, **248**, 5183–5187.
- 54 I. Hanukoglu, R. Rapoport, L. Weiner and D. Sklan, *Arch. Biochem. Biophys.*, 1993, **305**, 489–498.
- 55 R. Rapoport, D. Sklan and I. Hanukoglu, *Arch. Biochem. Biophys.*, 1995, **317**, 412–416.
- 56 I. Hanukoglu, *Drug Metab. Rev.*, 2006, **38**, 171–196.
- 57 I. A. Martsinkivichene, N. K. Chenas, I. Kulis and S. A. Usanov, *Biochemistry*, 1990, **55**, 1624–1631.
- 58 J. Marcinkeviciene, N. Cenas, J. Kulys, S. A. Usanov, N. M. Sukhova, I. S. Selezneva and V. F. Gryazev, *Biomed. Biochim. Acta*, 1990, **49**, 167–172.
- 59 T. M. Cho, R. L. Rose and E. Hodgson, *Drug Metab. Dispos.*, 2006, **34**, 176–183.
- 60 T. Shimada, D. Kim, N. Murayama, K. Tanaka, S. Takenaka, L. D. Nagy, L. M. Folkman, M. K. Foroozesh, M. Komori, H. Yamazaki and F. P. Guengerich, *Chem. Res. Toxicol.*, 2013, **26**, 517–528.
- 61 H. Kappus and H. Sies, *Experientia*, 1981, **37**, 1233–1241.
- 62 P. J. Thornalley, M. d'Arcy Doherty, M. T. Smith, J. V. Bannister and G. M. Cohen, *Chem.-Biol. Interact.*, 1984, **48**, 195–206.
- 63 S. P. de Visser and S. Shaik, *J. Am. Chem. Soc.*, 2003, **125**, 7413–7424.
- 64 G. Gueroff, J. W. Daly, D. M. Jerina, J. Renson, B. Witkop and S. Udenfriend, *Science*, 1967, **157**, 1524–1530.
- 65 D. M. Jerina and J. W. Daly, *Science*, 1974, **185**, 573–582.